

## Nickel nanoparticles supported on MOF-5: Synthesis and catalytic hydrogenation properties

Huahua Zhao<sup>a,b</sup>, Huanling Song<sup>a</sup>, Lingjun Chou<sup>a,\*</sup>

<sup>a</sup> State Key Laboratory for Oxo Synthesis and Selective Oxidation, Lanzhou Institute of Chemical Physics, Chinese Academy of Sciences, Lanzhou 730000, PR China

<sup>b</sup> Graduate School of Chinese Academy of Sciences, Beijing 100049, PR China

### ARTICLE INFO

#### Article history:

Received 24 August 2011

Accepted 17 October 2011

Available online 3 November 2011

#### Keywords:

Wet impregnation strategy

Ni@MOF-5

Crotonaldehyde

Hydrogenation

### ABSTRACT

Nickel nanoparticles (2–6 nm) were successfully deposited on MOF-5 ( $Zn_4O(BDC)_3$ , BDC = 1,4-benzenedicarboxylate) by a facile wet impregnation strategy to prepare Ni@MOF-5 employing Ni(acac)<sub>2</sub> (acac = acetylacetonate) as the precursor in absolute ethanol solvent owing to the sensitivity to the moisture of MOF-5. Ni@MOF-5 exhibited excellent catalytic activity for hydrogenation of C=C bond using crotonaldehyde as a probe molecule under mild reaction conditions (conversion > 90.0%, selectivity > 98.0%, 2.0 MPa, 100 °C, 40 min). In addition, the catalyst could be reused and the structure of MOF-5 framework was still maintained. Therefore, MOF-5 promised a novel candidate of support for hydrogenation catalyst.

© 2011 Elsevier B.V. All rights reserved.

### Introduction

In recent years, metal–organic frameworks (MOFs) have attracted considerable attention in the field of catalysis on account for their large specific surface areas and high porosities unparalleled so far by other traditional materials [1–3]. Owing to their low thermal stabilities (200–500 °C) [4–6], MOFs can be utilized for the reactions requiring mild conditions, such as Knoevenagel condensation, cyanosilylation of aldehyde, oxidation of olefin, transesterification and so on [7–11]. Despite many exciting achievements have been made recently, the area of MOF-based catalysis is still in its infancy [12,13].

One of the most representative MOFs is MOF-5 ( $Zn_4O(BDC)_3$ ) with BET surface area from 260 m<sup>2</sup>/g to 4400 m<sup>2</sup>/g based on the synthetic method and good thermal stability up to 400 °C [14]. Recently, its potential applications in gas storage (H<sub>2</sub> and CO<sub>2</sub>) and heterogeneous catalysis were intensively attracted to study [15–17]. In the field of catalysis, as an efficient catalyst, Ravon et al. and Phan et al. investigated the catalytic activity of MOF-5 over the alkylation reactions [17,18]. As the support for catalysts, MOF-5 was applied into some reactions, for example, hydrogenation, aerobic oxidation of alcohols and Sonogashira coupling reactions [19–21]. Especially, there was a little focus on MOF-5 for hydrogenation. Sabo et al. and Opelt et al. respectively reported that noble metal palladium loaded on MOF-5 by solution infiltration strategy and coprecipitation method to prepare the catalyst Pd@MOF-5, which showed high catalytic activity for

hydrogenation of C=C bond [21,22]. Fischer et al. deposited non-precious metal Cu and ZnO particles on MOF-5 by vapor deposition technique to synthesize Cu/ZnO@MOF-5, which displayed a good initial catalytic productivity in the hydrogenation of CO<sub>2</sub> [23]. In addition, nickel-based catalysts are extensively employed on various hydrogenations including the hydrogenation for C=C bond, which exhibit excellent and particular performance [24–26]. However, making use of MOF-5 as the support of nickel catalyst has not been well explored so far.

In the following, the wet impregnation strategy was successfully applied to prepare Ni@MOF-5 employing Ni(acac)<sub>2</sub> as the precursor, absolute ethanol as the solvent, and MOF-5 made-in-house with large surface area as the support. The catalytic activity of Ni@MOF-5 was explored on the hydrogenation for crotonaldehyde under mild conditions [27]. Furthermore, the reusability of the catalyst was also studied.

### Experimental

#### Catalyst preparation and characterization

All chemicals were received and directly used without further purification except crotonaldehyde purified by distillation. H<sub>2</sub>BDC was purchased from Merck-Schuchardt (Germany). Zinc nitrate hexahydrate ( $Zn(NO_3)_2 \cdot 6H_2O$ ) and nickel nitrate hexahydrate ( $Ni(NO_3)_2 \cdot 6H_2O$ ) were from Sinopharm Chemical Reagent Co., Ltd (China). *N,N*-dimethylformamide (DMF), triethylamine (TEA), trichloromethane (CHCl<sub>3</sub>), acetylacetone (Hacac), NaOH and ethanol were all from Tianjin Chemical Reagent Company (China).

\* Corresponding author. Tel.: +86 0931 4968136; fax: +86 0931 4968129.  
E-mail address: [lchou@licp.cas.cn](mailto:lchou@licp.cas.cn) (L. Chou).

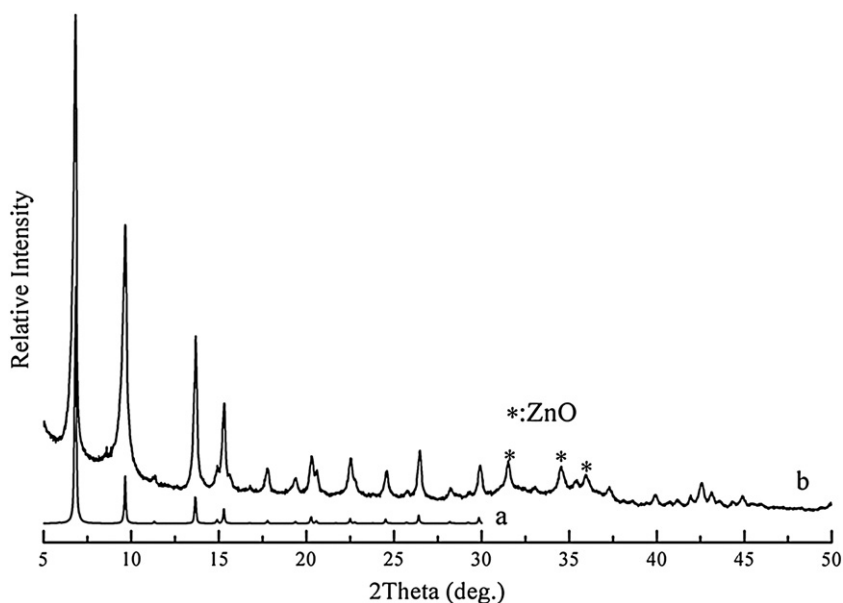


Fig. 1. The XRD patterns of MOF-5: (a) simulated; (b) as-synthesized.

$\text{Ni}(\text{acac})_2$  was prepared by grinding  $\text{Ni}(\text{NO}_3)_2 \cdot 6\text{H}_2\text{O}$ , NaOH and Hacac in ratio of 1:2:4 (mole ratio) for 15 min at room temperature, then drying under vacuum at 100 °C for 10 h to obtain the green powder in our experiment.

The support MOF-5 was prepared by direct mixing strategy described by Huang et al. with slight modifications [28]. Prior to prepare the catalyst, as-synthesized MOF-5 was calcinated in  $\text{N}_2$  flow at 250 °C for 6 h to remove the guest molecules from the pores.  $\text{Ni}(\text{acac})_2$  (1.0 g) was dissolved in ethanol (150.0 mL) to form a dark green solution at 60 °C. Subsequently, guest-free MOF-5 (2.0 g) was added into the solution under continuous agitation. The mixture was stirred for 12–15 h in air, and then filtered, dried under vacuum at 60 °C for 2 h to yield a green powder  $\text{Ni}(\text{acac})_2@$ MOF-5. Finally, the powder was directly reduced under  $\text{N}_2/\text{H}_2$  (4:1, v/v) flow at 340 °C for 3 h to obtain  $\text{Ni}@$ MOF-5 catalyst.

XRD patterns were measured on an X'Pert Pro multipurpose diffractometer (PANalytical) with Ni-filtered  $\text{Cu K}\alpha$  radiation ( $\lambda = 0.15046$  nm). Measurements were performed with a voltage of 40 kV, current setting of 40 mA and scan step size of 0.02°.

TEM was done on a JEM-2010 transmission electron microscope.

The nickel loadings of the catalyst were determined by atomic adsorption spectroscopy (AAS) 18080 from Hitachi Company of Japan.

The  $\text{N}_2$  adsorption–desorption isotherms were performed with a Quantachrome autosorb iQ gas-sorption apparatus at  $-196$  °C. All samples were outgassed under vacuum at 250 °C for 4 h prior to the measurements.

### Hydrogenation

The liquid phase hydrogenation reaction was carried out in a 300 mL stainless steel autoclave at 100 °C under 2.0 MPa  $\text{H}_2$ , and with a stirring speed of 500 rpm. For a typical experiment, 0.85 g of the catalyst, 90 mL of ethanol, and 10 mL of the purified crotonaldehyde were loaded. The reaction products were identified by a GC-MS 5973 equipment from Agilent Technology Company and analyzed by a gas chromatograph with a SE54 capillary column and a flame ionization detector.

The recycle of the catalyst: After the first run, the catalyst was collected by configuration, dried under vacuum at 60 °C, then reduced under  $\text{N}_2/\text{H}_2$  (4:1, v/v) flow at 340 °C for 30 min and utilized for the next run.

## Results and discussion

### Characterization of the catalysts

Fig. 1 shows the XRD pattern of MOF-5. It was clearly seen that the four main diffraction peaks (6.8°, 9.7°, 13.7° and 15.4°) of the as-synthesized product were in good agreement with that of the simulated one [29], suggesting that the as-synthesized product had the MOF-5 structure. Furthermore, the sharp peaks indicated that MOF-5 had good crystallinity. Additionally, the small peaks (31.5°, 34.6° and 36.1°) suggested that MOF-5 framework was entrapped by a trace amount of ZnO [16].

The XRD patterns of the catalysts at different steps are presented in Fig. 2. It is clearly seen that two extra small peaks (10.4° and 12.4°) appeared in the XRD patterns of the catalyst after loading with  $\text{Ni}(\text{acac})_2$ , which was probably owing to the symmetry of MOF-5 structure changing from cubic to trigonal [30] during the preparation of the catalyst. However, the four main peaks of MOF-5 were basically maintained. The two extra peaks disappeared after the catalyst reduced, suggesting that the MOF-5 structure was recovered, although the peak intensity of ZnO became a little stronger. Furthermore, a small diffraction peak (44.5°) was attributable to metallic Ni in the XRD patterns of the catalyst after reduction indicating that Ni particles were probably well dispersed on MOF-5. Fig. 2d–f shows the XRD patterns of the catalyst during the retest runs. The four main peaks were maintained implying that the MOF-5 structure was persevered well after the retest runs.

The TEM images of the reduced and reacted catalysts are shown in Fig. 3. It could be seen from Fig. 3b that the crystal size of MOF-5 was uniformly about 60–80 nm, which was consistent with the results Huang et al. reported [28]. The grain size of Ni was 2–6 nm, which was larger than the pore diameter (1.02 nm) of MOF-5. Thus, nickel nanoparticles were distributed on the outer surface of MOF-5 support. Due to the small grain size, the XRD diffraction peak intensity of Ni was very small. It was also seen that the Ni nanoparticles had a little agglomeration on the support.

The BET specific surface areas and pore volumes of the catalysts are presented in Table 1. The BET surface areas of MOF-5 could attain 822.0  $\text{m}^2/\text{g}$  based on the  $\text{N}_2$  adsorption–desorption measurements. The BET surface area greatly decreased from 821.6  $\text{m}^2/\text{g}$  to 619.9  $\text{m}^2/\text{g}$  and the micropore volume decreased from 0.28  $\text{cm}^3/\text{g}$  to 0.22  $\text{cm}^3/\text{g}$  after reduction, probably due to the destructive influence

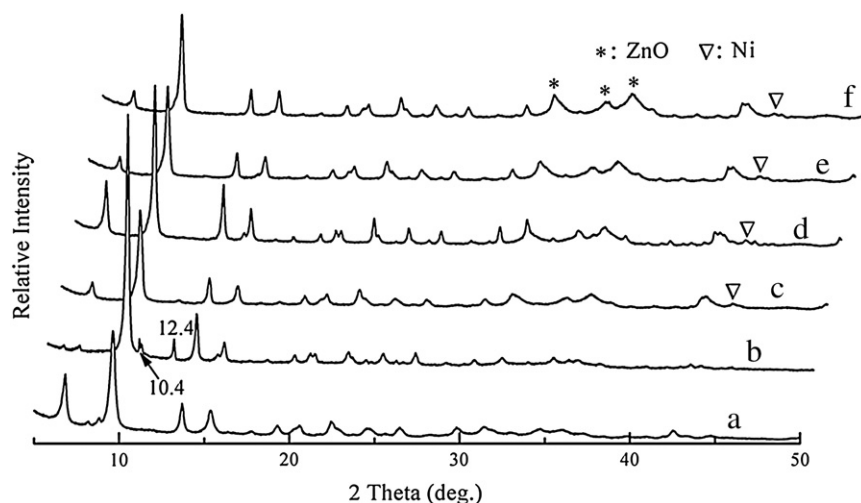


Fig. 2. The XRD patterns of the catalysts: (a) MOF-5; (b) Ni(acac)<sub>2</sub>@MOF-5; (c) fresh Ni@MOF-5; (d) Ni@MOF-5 1st run; (e) Ni@MOF-5 2nd run; (f) Ni@MOF-5 3rd run.

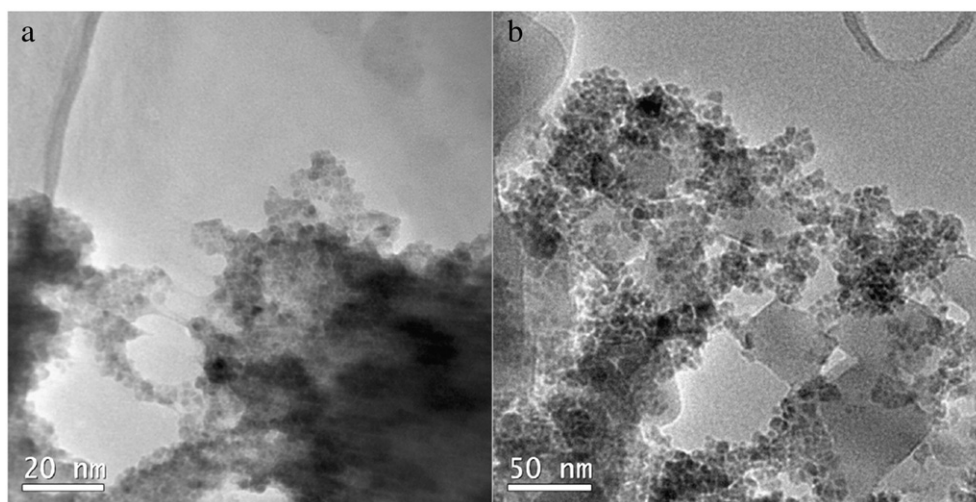


Fig. 3. TEM images of the catalyst after: (a) reduced; (b) reaction.

of the trace water in ethanol during the catalyst preparation and the nickel nanoparticles which may take up partial pore channels of the framework. After reaction, the BET surface area of MOF-5 decreased largely from 619.9 m<sup>2</sup>/g to 479.3 m<sup>2</sup>/g and the volume of micropore reduced from 0.22 cm<sup>3</sup>/g to 0.17 cm<sup>3</sup>/g, whereas the total pore volume slightly decreased (0.34 → 0.32 cm<sup>3</sup>/g), indicating that partial micropores were probably taken up by some small reaction or product molecules. The BET surface area and pore volume of MOF-5 had no further decrease during the retest runs, which suggested that the

MOF-5 structure was not significantly influenced by the reaction conditions. In addition, the pore diameter of the support was 1.02 nm, smaller than the size of Ni nanoparticles, implying that nickel nanoparticles probably bond on the outer surface of MOF-5 support as described above.

#### Catalytic activity

The hydrogenation of crotonaldehyde (Scheme 1) was chosen to test the activity of Ni@MOF-5, because hydrogenation of unsaturated aldehydes was a typical model reaction to establish the relations between selectivity and catalyst structures [31]. For the hydrogenation of crotonaldehyde on the catalyst Ni@MOF-5 in our study, butyraldehyde was

Table 1

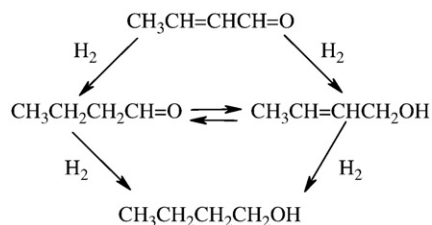
The pore properties of the catalysts at different steps.

Catalysts	S <sub>BET</sub> (m <sup>2</sup> /g)	V <sub>p</sub> -SF <sup>a</sup> (cm <sup>3</sup> /g)	V <sub>p</sub> -DFT <sup>b</sup> (cm <sup>3</sup> /g)	D <sub>p</sub> -DFT <sup>c</sup> (nm)
MOF-5	821.6	0.28	0.48	1.02
Ni@MOF-5 reduced	619.9	0.22	0.34	1.02
Ni@MOF-5 1st run	479.3	0.17	0.32	1.02
Ni@MOF-5 2nd run	353.3	0.12	0.23	1.02
Ni@MOF-5 3rd run	441.5	0.15	0.29	1.02
Ni@SiO <sub>2</sub>	172.2	–	0.49	11.28

<sup>a</sup> Pore volumes of the products calculated with the Saito–Foley (SF) method.

<sup>b</sup> Pore volumes of the products calculated with non local density functional theory (NLDFT).

<sup>c</sup> Pore diameters of the products calculated with non local density functional theory (NLDFT).



Scheme 1. The products of selective hydrogenation for crotonaldehyde.

**Table 2**

The activity and selectivity of different catalysts over the hydrogenation of crotonaldehyde.

Catalysts	Ni loadings	Reaction time (min)	C <sub>CROL</sub> <sup>a</sup> (%)	S <sub>BRAD</sub> <sup>b</sup> (%)	TOF <sub>CROL</sub> (h <sup>-1</sup> )	TOF <sub>BRAD</sub> (h <sup>-1</sup> )
MOF-5	–	60	11.88	1.18	–	–
Ni@MOF-5	7.4	40	91.59	98.30	154.6	152.0
		60	99.45	90.11	111.9	100.8
Ni/SiO <sub>2</sub>	28.0	40	83.06	94.38	73.9	69.8

<sup>a</sup> CROL for crotonaldehyde.

<sup>b</sup> BRAD for butyraldehyde.

the main product with a small amount of butanol and other by-products whereas, no crotyl alcohol was detected.

The results of hydrogenation for crotonaldehyde are summarized in Table 2. The yield of butyraldehyde was only 0.14% when the reaction was conducted in the presence of MOF-5 at 100 °C for 60 min, illustrating that MOF-5 itself had little catalytic performance for hydrogenation. Using the same amount of the catalyst Ni@MOF-5, the conversion of crotonaldehyde increased to 91.59% with high selectivity of butyraldehyde (98.30%) at 100 °C for 40 min. However, crotonaldehyde was almost completely converted (99.45%) with slight decrease of selectivity (90.11%) after 60 min.

The catalytic activity of Ni@MOF-5 was also compared with that of the industrial catalyst Ni/SiO<sub>2</sub> containing 28.0 wt.% Ni with BET surface area of 172.2 m<sup>2</sup>/g. Ni/SiO<sub>2</sub> was treated under the same conditions as Ni(acac)<sub>2</sub>@MOF-5 prior to the hydrogenation reaction. By contrast, Ni/SiO<sub>2</sub> with the catalytic amount (0.43 g) exhibited only 83.06% conversion with 94.38% selectivity of butyraldehyde at 100 °C for 40 min. In terms of the turnover of frequency (TOF, denoted as the mole content of crotonaldehyde converted over per mole Ni per hour), Ni@MOF-5 (154.6 h<sup>-1</sup>) showed a remarkably higher activity than that of Ni/SiO<sub>2</sub> (73.9 h<sup>-1</sup>). Consequently, Ni@MOF-5 had a high catalytic activity and selectivity for C=C bond hydrogenation. The superior activity of Ni@MOF-5 might be mainly attributed to the larger nickel surface area resulted from the small nickel nanoparticles supported on the support MOF-5.

#### The reusability of Ni@MOF-5

To find out if the catalyst has retained its initial catalytic activity and its structure, the reusability of the catalyst was carried. Fig. 4

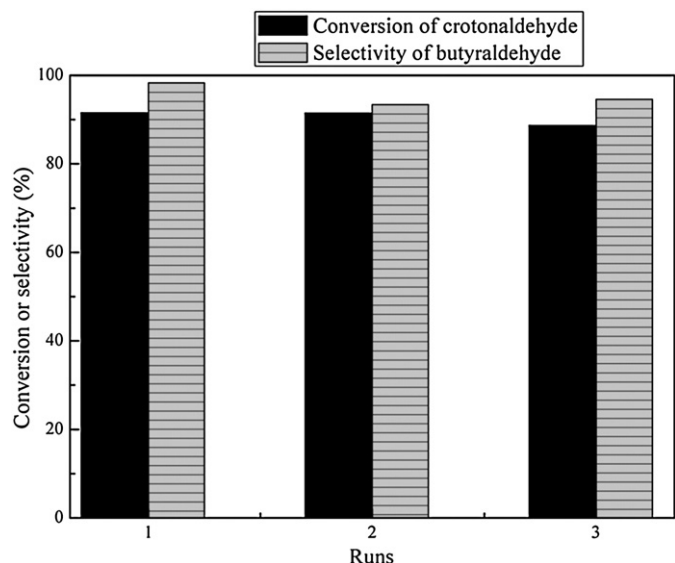


Fig. 4. The activity and selectivity for hydrogenation of crotonaldehyde in the three retest runs.

describes the activity and selectivity of the catalyst for three retest runs with the reaction time 60 min. In the first run, the conversion of crotonaldehyde was up to 99.45% with high butyraldehyde selectivity of 90.11%. In the second run, the conversion of crotonaldehyde maintained at 91.49%, whereas the selectivity of butyraldehyde increased to 93.39%. In the third hydrogenation, the conversion of crotonaldehyde decreased to 88.73% with the selectivity almost constant at 93.40%. Fortunately, the structure of MOF-5 was preserved well throughout the reaction according to the XRD patterns of the catalysts. Thus, the catalyst could be reused for several times with some degree of reduced catalytic performance.

#### Conclusions

In summary, Ni@MOF-5 (7.4 wt.% Ni) was successfully obtained by wet impregnation strategy to deposit nickel on MOF-5 framework. The nickel nanoparticles (2–6 nm) were probably located on the outer surface of the MOF-5 contributing to its small pore diameter (1.02 nm). Ni@MOF-5 displayed much higher catalytic activity in comparison with that of the industrial catalyst Ni/SiO<sub>2</sub>. Furthermore, the catalyst can be reused for several times with the preservation of MOF-5 structure. Thus, MOF-5 promised a novel candidate of support for hydrogenation catalyst. Current research may be well transferable to load some active components (Pt, Ag and Au) on other robust MOFs in this reaction, such as MIL series.

#### Acknowledgement

We gratefully acknowledge the financial support of the State Key Laboratory for Oxo Synthesis and Selective Oxidation of China.

#### References

- [1] A. Henschel, K. Gedrich, R. Kraehnert, S. Kaskel, Catalytic properties of MIL-101, Chem. Commun. (2008) 4192–4194.
- [2] N. Maksimchuk, M. Timofeeva, M. Melgunov, A. Shmakov, Y. Chesalov, D. Dybtsev, V. Fedin, O. Kholdeeva, Heterogeneous selective oxidation catalysts based on coordination polymer MIL-101 and transition metal-substituted polyoxometalates, J. Catal. 257 (2008) 315–323.
- [3] S. Proch, J. Herrmannsdörfer, R. Kempe, C. Kern, A. Jess, L. Seyfarth, J. Senker, Pt@MOF-177: Synthesis, Room-Temperature Hydrogen Storage and Oxidation Catalysis, Chem. Eur. J. 14 (2008) 8204–8212.
- [4] N.V. Maksimchuk, K.A. Kovalenko, S.S. Arzumanov, Y.A. Chesalov, M.S. Melgunov, A.G. Stepanov, V.P. Fedin, O.A. Kholdeeva, Hybrid Polyoxotungstate/MIL-101 Materials: Synthesis, Characterization, and Catalysis of H<sub>2</sub>O<sub>2</sub>-Based Alkene Epoxidation, Inorg. Chem. 49 (2010) 2920–2930.
- [5] K. Schlichte, T. Kratzke, S. Kaskel, Improved synthesis, thermal stability and catalytic properties of the metal-organic framework compound Cu<sub>3</sub>(BTC)<sub>2</sub>, Microporous Mesoporous Mater. 73 (2004) 81–88.
- [6] C. Serre, F. Millange, C. Thouvenot, M. Nogues, G. Marsolier, D. Louër, G. Férey, Very Large Breathing Effect in the First Nanoporous Chromium(III)-Based Solids: MIL-53 or Cr<sup>III</sup>(OH)·{O<sub>2</sub>C–C<sub>6</sub>H<sub>4</sub>–CO<sub>2</sub>}·{HO<sub>2</sub>C–C<sub>6</sub>H<sub>4</sub>–CO<sub>2</sub>H}<sub>x</sub>·H<sub>2</sub>O, J. Am. Chem. Soc. 124 (2002) 13519–13526.
- [7] S. Hasegawa, S. Horike, R. Matsuda, S. Furukawa, K. Mochizuki, Y. Kinoshita, S. Kitagawa, Three-Dimensional Porous Coordination Polymer Functionalized with Amide Groups Based on Tridentate Ligand: Selective Sorption and Catalysis, J. Am. Chem. Soc. 129 (2007) 2607–2614.
- [8] M. Fujita, Y.J. Kwon, S. Washizu, K. Ogura, Preparation, Clathration Ability, and Catalysis of a Two-Dimensional Square Network Material Composed of Cadmium(II) and 4,4'-Bipyridine, J. Am. Chem. Soc. 116 (1994) 1151–1152.
- [9] Y. Lu, M. Tonigold, B. Bredenkötter, D. Volkmer, J. Hitzbleck, G. Langstein, A Cobalt(II)-containing Metal-Organic Framework Showing Catalytic Activity in Oxidation Reactions, Z. Anorg. Allg. Chem. 634 (2008) 2411–2417.
- [10] J.S. Seo, D. Whang, H. Lee, S.I. Jun, J. Oh, Y.J. Jeon, K. Kim, A homochiral metal-organic porous material for enantioselective separation and catalysis, Nature 404 (2000) 982–986.
- [11] R.-Q. Zou, H. Sakurai, Q. Xu, Preparation, adsorption properties, and catalytic activity of 3D porous metal-organic frameworks composed of cubic building blocks and alkali-metal ions, Angew. Chem. Int. Ed. 45 (2006) 2542–2546.
- [12] D. Farrusseng, S. Aguado, C. Pinel, Metal-Organic Frameworks: Opportunities for Catalysis, Angew. Chem. Int. Ed. 48 (2009) 7502–7513.
- [13] J. Lee, O.K. Farha, J. Roberts, K.A. Scheidt, S.T. Nguyen, J.T. Hupp, Metal-organic framework materials as catalysts, Chem. Soc. Rev. 38 (2009) 1450–1459.
- [14] S.S. Kaye, A. Dailly, O.M. Yaghi, J.R. Long, Impact of Preparation and Handling on the Hydrogen Storage Properties of Zn<sub>4</sub>O(1,4-benzenedicarboxylate)<sub>3</sub> (MOF-5), J. Am. Chem. Soc. 129 (2007) 14176–14177.

- [15] C.-M. Lu, J. Liu, K. Xiao, A.T. Harris, Microwave enhanced synthesis of MOF-5 and its CO<sub>2</sub> capture ability at moderate temperatures across multiple capture and release cycles, *Chem. Eng. J.* 156 (2010) 465–470.
- [16] B. Chen, X. Wang, Q. Zhang, X. Xi, J. Cai, H. Qi, S. Shi, J. Wang, D. Yuan, M. Fang, Synthesis and characterization of the interpenetrated MOF-5, *J. Mater. Chem.* 20 (2010) 3758–3767.
- [17] U. Ravon, M.E. Domine, C. Gaudillère, A. Desmartin-Chomel, D. Farrusseng, MOFs as acid catalysts with shape selectivity properties, *New J. Chem.* 32 (2008) 937–940.
- [18] N.T.S. Phan, K.K.A. Le, T.D. Phan, MOF-5 as an efficient heterogeneous catalyst for Friedel–Crafts alkylation reactions, *Appl. Catal., A: General* 382 (2010) 246–253.
- [19] S. Gao, N. Zhao, M. Shu, S. Che, Palladium nanoparticles supported on MOF-5 A highly active catalyst for a ligand- and copper-free Sonogashira coupling reaction, *Appl. Catal., A: General* 388 (2010) 196–201.
- [20] T. Ishida, M. Nagaoka, T. Akita, M. Haruta, Deposition of Gold Clusters on Porous Coordination Polymers by Solid Grinding and Their Catalytic Activity in Aerobic Oxidation of Alcohols, *Chem. Eur. J.* 14 (2008) 8456–8460.
- [21] M. Sabo, A. Henschel, H. Fröde, E. Klemm, S. Kaskel, Solution infiltration of palladium into MOF-5: synthesis, physisorption and catalytic properties, *J. Mater. Chem.* 17 (2007) 3827–3832.
- [22] S. Opelt, S. Türk, E. Dietzsch, A. Henschel, S. Kaskel, E. Klemm, Preparation of palladium supported on MOF-5 and its use as hydrogenation catalyst, *Catal. Commun.* 9 (2008) 1286–1290.
- [23] M. Müller, S. Hermes, K. Kähler, M.W.E. van den Berg, M. Muhler, R.A. Fischer, Loading of MOF-5 with Cu and ZnO Nanoparticles by Gas-Phase Infiltration with Organometallic Precursors: Properties of Cu/ZnO@MOF-5 as Catalyst for Methanol Synthesis, *Chem. Mater.* 20 (2008) 4576–4587.
- [24] S.Y. Chin, F.J. Lin, A.N. Ko, Vapour Phase Hydrogenation of Cinnamaldehyde over Ni/gamma-Al<sub>2</sub>O<sub>3</sub> Catalysts: Interesting Reaction Network, *Catal. Lett.* 132 (2009) 389–394.
- [25] Y. Qian, S.Q. Liang, T.H. Wang, Z.B. Wang, W. Xie, X.L. Xu, Enhancement of pyrolysis gasoline hydrogenation over Zn- and Mo-promoted Ni/gamma-Al<sub>2</sub>O<sub>3</sub> catalysts, *Catal. Commun.* 12 (2011) 851–853.
- [26] E. Vesselli, J. Schweicher, A. Bundhoo, A. Frennet, N. Kruse, Catalytic CO<sub>2</sub> Hydrogenation on Nickel: Novel Insight by Chemical Transient Kinetics, *J. Phys. Chem. C* 115 (2011) 1255–1260.
- [27] C.G. Raab, J.A. Lercher, Activity and selectivity of PtNi/TiO<sub>2</sub> catalysts for hydrogenation of crotonaldehyde, *Catal. Lett.* 18 (1993) 99–109.
- [28] L. Huang, H. Wang, J. Chen, Z. Wang, J. Sun, D. Zhao, Y. Yan, Synthesis, morphology control, and properties of porous metal–organic coordination polymers, *Microporous Mesoporous Mater.* 58 (2003) 105–114.
- [29] J.L.C. Rowsell, E.C. Spencer, J. Eckert, J.A.K. Howard, O.M. Yaghi, Gas Adsorption Sites in a Large-Pore Metal–Organic Framework, *Science* 309 (2005) 1350–1354.
- [30] J. Hafizovic, M. Bjørgen, U. Olsbye, P.D.C. Dietzel, S. Bordiga, C. Prestipino, C. Lamberti, K.P. Lillerud, The Inconsistency in Adsorption Properties and Powder XRD Data of MOF-5 Is Rationalized by Framework Interpenetration and the Presence of Organic and Inorganic Species in the Nanocavities, *J. Am. Chem. Soc.* 129 (2007) 3612–3620.
- [31] H. Noller, W.M. Lin, Activity and Selectivity of Ni-Cu/Al<sub>2</sub>O<sub>3</sub> Catalysts for Hydrogenation of Crotonaldehyde and Mechanism of Hydrogenation, *J. Catal.* 85 (1984) 25–30.